



## Heavy metals removal from aqueous solution using magnetite Dowex 50WX4 resin nanocomposite

Lasheen M.R.<sup>a</sup>, Iman Y. El-Sherif<sup>a</sup>, Shaimaa T. El-Wakeel<sup>a,\*</sup>,  
Dina Y. Sabry<sup>b</sup>, El-Shahat M.F.<sup>b</sup>

<sup>a</sup> Water Pollution Research Department, Environmental Research Division, National Research Centre, 33- El Buhoth St, Dokki, Cairo, 12311, Egypt

<sup>b</sup> Faculty of Science, Ain Shams University, Khalifa El-Maamonst, Abbassia Sq., 11566, Cairo, Egypt.

Received 13 Jul 2016,  
Revised 23 Nov 2016,  
Accepted 05 Dec 2016

### Keywords

- ✓ Heavy metals
- ✓ Magnetite
- ✓ Resin
- ✓ Adsorption.

Shaimaa T. El-Wakeel  
[shaimaa\\_tw@yahoo.com](mailto:shaimaa_tw@yahoo.com)  
+ 202 33371211

### Abstract

Magnetite –Dowex 50WX4 (Mag-Dow) nanocomposite was synthesized, characterized and tested for heavy metal ions (Cr (VI), Ni<sup>2+</sup>, Cu<sup>2+</sup>, Cd<sup>2+</sup> and Pb<sup>2+</sup>) removal. Transmission Electron Microscopy (TEM) results showed the formation of nanoparticles of size ranging from 2-10 nm. Adsorption experiments in batch mode were conducted using the developed nanocomposite. Different factors affecting the adsorption process like reaction time, initial metals concentration, pH and adsorbent dose were investigated to optimize the operation conditions for the composite nanoparticles. The adsorption capacity of the composite was found to increase by time and adsorption attains equilibrium in 30 min. The highest maximum adsorption capacity obtained from Langmuir isotherm model was 416 mg/g for Cu<sup>2+</sup> ions and the adsorption process is well fitted by pseudo-second order kinetic model. The desorption efficiency for different metals used was found to be 96 % of the prepared adsorbent suggest that the prepared composite is as an effective tool for removal of the selected heavy metals.

## 1. Introduction

Heavy metals such as lead, cadmium, copper, nickel and mercury are distributed throughout the environment as a result of soil erosion, industrial and agricultural processes. The poisoning effects of heavy metals are due to their interference with the biochemistry of the body causing various diseases [1]. Different techniques were adopted for metals removal and water treatment such as membrane separation [2,3], coagulation, flocculation [4], chemical treatment [5], filtration [6] and adsorption [7,8], have been developed. Adsorption is one of the methods that used for heavy metals removal and has advantages over the other methods because of simple design, low cost and no sludge formation.

Different natural materials such as clay, seaweed and biomass, and synthetic materials like activated carbon, resin, and mesoporous silica [9] have been used to remove heavy metals by adsorption. Heavy metals removal by chelating resins is another promising method and many studies reported the use of different chelating resins [10,11]. The limitations on the use of ion exchange are primarily high cost and the requirements for appropriate pretreatment systems. Recently, the preparation and application of iron oxides specially magnetite nanoparticles for metals removal have been investigated, due to their nano size, magnetic separation and the easy of synthesis, coating and modification [5,6,12,13]. However, magnetic nanoparticles lose some of magnetization due to air oxidation. Magnetite nanoparticles coating with inorganic shell, like silica [7,14] and carbon [8,15] have been reported and were capable to improve its chemical stability. Recently, the use of magnetic resins in heavy metals removal has been investigated [9,16].

Magnetic ion exchange resins were applied firstly in 1995 for the removal of natural organic matter [7,17]. Magnetic resins are easily collected from solutions through applying an external magnetic field and have a higher uptake capacity compared to the free resin magnetic nanoparticles [10,8]. In this work, the cross-linked magnetite Dowex 50 W X resin nanocomposite was prepared using co-precipitation method. The prepared nanocomposites were characterized and tested for heavy metals (Cr(VI), Ni<sup>2+</sup>, Cu<sup>2+</sup>, Cd<sup>2+</sup> and Pb<sup>2+</sup>) removal.

## 2. Experimental

### 2.1. Synthesis of magnetite–Dowex (Mag-Dow) nanocomposite

Dowex 50 WX4 resin was obtained from Fluka Co. The properties of the resin are given in Table 1. A suspension of Dowex 50 WX4 resin in a solution of  $\text{FeCl}_3 \cdot 6\text{H}_2\text{O}$  (2M) and  $\text{FeCl}_2 \cdot 4\text{H}_2\text{O}$  (1M) was prepared. The amount of resin was adjusted in order to obtain 1:1 weight ratios of magnetite: resin and stirring at a rate of 200 rpm at 80°C. Ammonium hydroxide solution was added to precipitate nano magnetite at pH 10-12. The obtained precipitate was dried in an oven at 80°C after washing with deionized water.

**Table 1.** Characteristic data of tested Dowex 50WX4 resin

<b>Type</b>	Strong acid cation exchanger Dowex 50W-X4
<b>Active group</b>	Sulfonic acid
<b>Ionic forms as shipped</b>	$\text{H}^+$
<b>Total exchange capacity (eq/L)</b>	1.1

### 2.2. Characterization of adsorbent

The structural characterization of the prepared Mag-Dow was conducted by powder X-ray diffraction spectrometry (XRD) using Bruker D8 advance instrument between 5 and 80° (2 $\theta$ ) at a scanning rate of 4°/min. Morphology and size were investigated by Transmission Electron Microscopy (TEM) using JOEL JEM (1230) electron microscope instrument. Gas adsorption analyzer with Brunauer-Emmett-Teller (BET) method (Quanta chrome NOVA automated gas sorption system sorb-1.12) was used for the surface area determination where  $\text{N}_2$  gas was used as adsorbate at 77K. The functional groups of different adsorbents were identified by Fourier Transform Infrared Spectroscopy (FTIR) analysis using FTIR-6100 (JASCO- Japan) instrument via the KBr pressed disc method, in a range starting from 400 to 4000  $\text{cm}^{-1}$  wavenumbers. Magnetic properties were measured in the solid state using a Vibrating Sample Magnetometer (VSM). The saturation magnetization value was determined from the plateau region of the magnetic flux density of a solid sample at 8000.

### 2.3. Adsorption studies

The adsorption behavior of the prepared Mag-Dow nanocomposite for metal ions ( $\text{Cr(VI)}$ ,  $\text{Ni}^{2+}$ ,  $\text{Cu}^{2+}$ ,  $\text{Cd}^{2+}$  and  $\text{Pb}^{2+}$ ) was investigated by means of batch experiments at room temperature. Batch adsorption experiments were conducted at 20 mg/L of each metal ion solution using different doses of the adsorbent ranged from 0.1 to 4 g/L. The adsorption of metal ions by the prepared nanocomposite was investigated in the pH range of 2–7. The highest tested pH value for each metal in the experiments was prior to the pH of metals precipitation which are (pHs 5.5, 7.5, 5.5, 7 and 6.5 for  $\text{Cr(VI)}$ ,  $\text{Ni}^{2+}$ ,  $\text{Cu}^{2+}$ ,  $\text{Cd}^{2+}$  and  $\text{Pb}^{2+}$  respectively). The solution pH was adjusted by 0.1 M NaOH and 0.1M  $\text{HNO}_3$ . Samples were shaken in a rotary shaker at 200 rpm at different contact times from 5 to 140 min.

The equilibrium adsorption capacity,  $q_e$  (mg /g), of metal was calculated using the mass balance, according to the following equation:

$$q_e = (C_o - C_e) V/m \quad (1)$$

Where V is the sample volume (L), m is the mass of the adsorbents (g),  $C_o$  is the initial metal ion concentration (mg/L), and  $C_e$  is the equilibrium concentration of metal ion in the solution (mg/L).

The concentration of metal ions in the solution was determined according to APHA [19] using Atomic Absorption Spectrometer (Varian Spectra AAS 220) with graphite furnace accessory and equipped with deuterium arc background corrector. The precision of the metal measurement was determined by analyzing in triplicate.

### 2.4. Desorption of metal ions and reusability of adsorbents

In this experiment, desorption of metals from metal-loaded nanoadsorbents was performed by adding a stripping solution of 2M NaCl and 1M NaOH mixture and stirred at 200rpm for 2h and the final metals concentration was determined. After each cycle of adsorption–desorption the nanoadsorbent was washed with distilled water then dried and reconditioned for adsorption in the succeeding cycle. The adsorption–desorption cycles were repeated consecutively five times to determine the reusability of sorbents.

### 3. Results and discussion

#### 3.1. Adsorbent characterization

TEM image of Mag-Dow nanocomposite (Fig. 1) indicates the homogeneity of the colloid and it is free of agglomeration. Most individual particles have a size ranging within 2–10 nm.

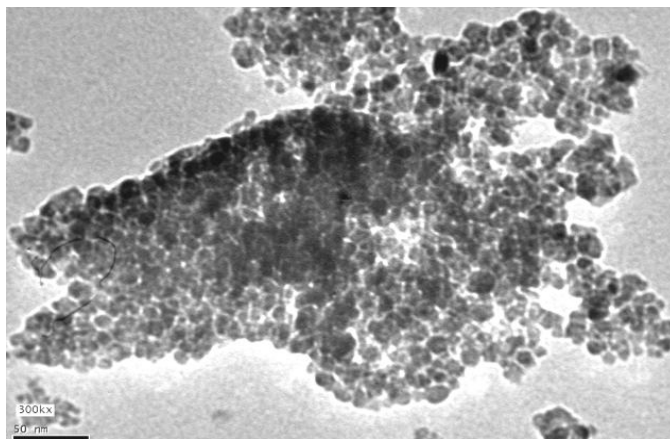


**Figure 1:** TEM image of Mag-Dow nanocomposite

XRD pattern (Fig. 2) shows the broad peak at  $2\theta$  of  $35.6^\circ$  indicates the presence of magnetite lattice planes in addition to resin peaks of  $2\theta$  range within  $10\text{--}30^\circ$ .

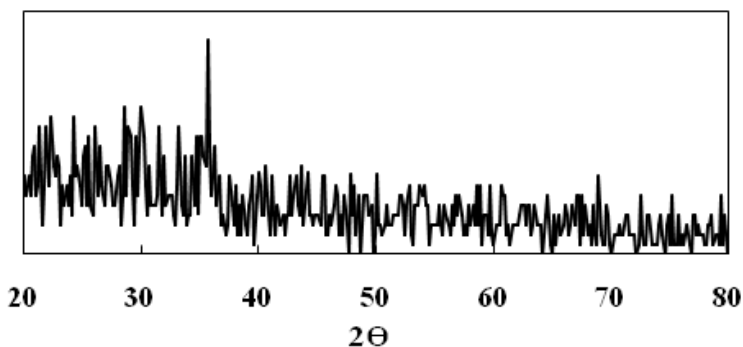


**Figure 2:** XRD pattern of Mag-Dow nanocomposite

FTIR chart for the prepared composite illustrates the characteristic absorption peak at  $537\text{ cm}^{-1}$  of Fe–O. Peaks at  $3779.8, 2925, 1407$  and  $1098\text{ cm}^{-1}$  in pure resin (Fig. 3.) were shifted to  $3389, 2919, 1402$  and  $1095\text{ cm}^{-1}$  in Mag-Dow nanocomposite chart which indicates mixing between both nano magnetite and resin.

The surface area of pure resin is  $72.2\text{ m}^2/\text{g}$  with total pore volume  $0.02\text{ cm}^3/\text{g}$ . In the prepared composite the surface area increased to  $160.2\text{ m}^2/\text{g}$  and total pore volume of  $0.067\text{ cm}^3/\text{g}$  with average pore size  $16\text{ \AA}$ .

The hysteresis curve (Fig. 4) for the composite magnetization measurement shows that the saturation magnetization was found to be  $50.1\text{ emu/g}$ . The saturation magnetization of the composite is lower than the values of the bulk and the prepared nano magnetite (stated in another work) which are  $92$  and  $58.2\text{ emu/g}$ . It could be attributed to the crystalline disorder within the surface layer [20] and the capping of some magnetic iron sites by resin. Generally, smaller magnetite cause decrease the magnetic moment.

#### 3.2. Effect of time and initial metal concentration

Fig. 5. shows the effect of contact time on the removal of metal ions ( $\text{Cr(VI)}$ ,  $\text{Ni}^{2+}$ ,  $\text{Cu}^{2+}$ ,  $\text{Cd}^{2+}$  and  $\text{Pb}^{2+}$ ) using the composite at initial metal concentration of  $20\text{ mg/L}$ . The results indicate that the removal percentage of metal ions increased with time increasing and the equilibrium for all metal ions was reached after 30 min. The composite adsorbs metals in order  $\text{Cu}^{2+} > \text{Cr(VI)} > \text{Cd}^{2+} > \text{Ni}^{2+} > \text{Pb}^{2+}$ . The removal percentages were increased compared to the

adsorption on Dowex50WX4 resin alone and equilibrium reached faster. Pehlivan and Altun [21] studied the removal of metal ions by Dowex resin alone and concluded that the metal ions removal was increased with time and the equilibrium was obtained at 70 min for  $\text{Cu}^{2+}$ ,  $\text{Zn}^{2+}$ ,  $\text{Pb}^{2+}$  and 60 min for  $\text{Ni}^{2+}$  and  $\text{Cd}^{2+}$  at initial concentration of 100 mg/l for the tested metals.

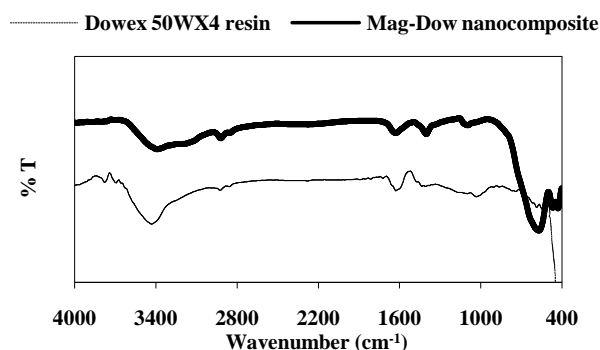


Figure 3: FTIR charts of Dowex 50WX4 and mag-Dow nanocomposite

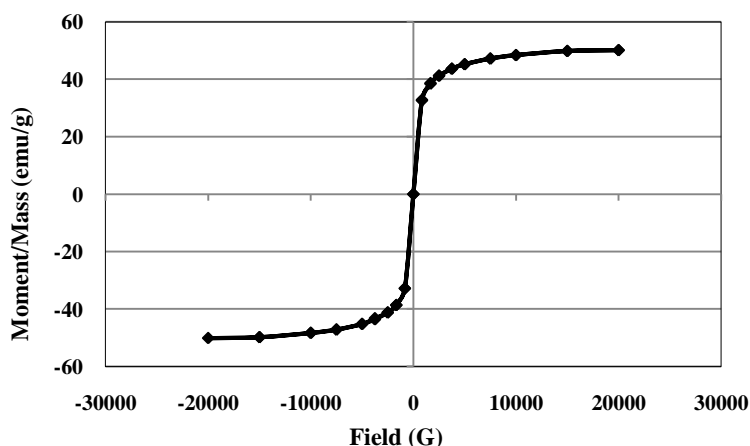


Figure 4 :VSM chart of Mag-Dow nanocomposite

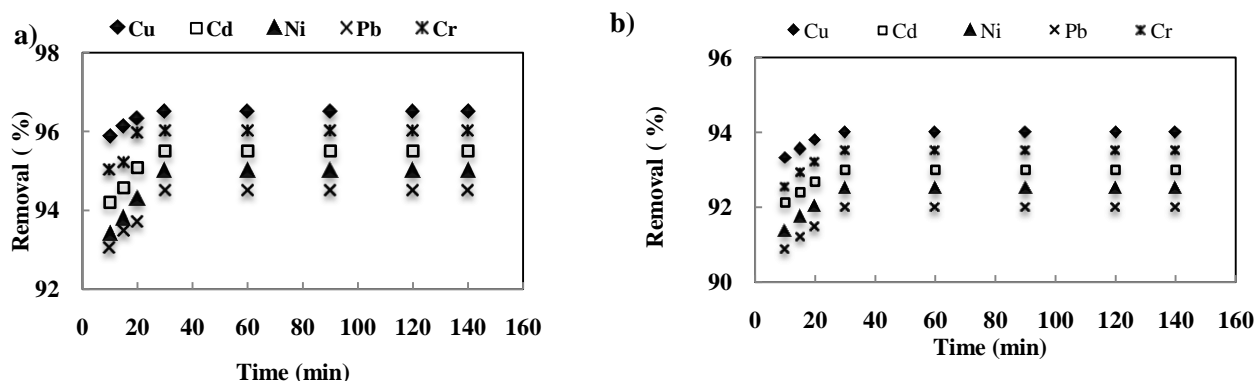


Figure 5: Effect of contact time on metals removal by Mag-Dow nanocomposite at initial metals concentration of (a) 20 mg/L (b) 100 mg/L.

The prepared composite have a large surface area and magnetic properties from the presence of nano magnetite and show effective adsorption for two difficult removable metals cadmium and nickel. The removal percentages were 97.5, 97, 96, 95 and 94.5 % for metal ions  $\text{Cu}^{2+}$ ,  $\text{Cr(VI)}$ ,  $\text{Cd}^{2+}$ ,  $\text{Ni}^{2+}$  and  $\text{Pb}^{2+}$  respectively, using the composite. Adsorption affinity of cadmium and nickel increased using Dowex 50WX4 resin alone, therefore using the resin compositing with magnetite improved magnetite ability for cadmium and nickel adsorption and increased

the ability of metals adsorption on resin at high concentrations. Metals adsorption percentages decrease with increasing the initial metals concentration to 100 mg/L. The adsorption decrease at higher metals concentration may be due to lack of the free high energy sites.

### 3.3. Effect of pH

Retention of metals on the prepared composite was studied at initial metal concentration of 20 mg/L and shown in Fig.6. The maximum removal percentage for  $\text{Cu}^{2+}$  attained to 99 using the composite at pH 5. For ions  $\text{Cr(VI)}$ ,  $\text{Ni}^{2+}$ ,  $\text{Cd}^{2+}$  and  $\text{Pb}^{2+}$  the removal percentage attained to 98, 97, 97.6 and 96% at pHs of 5.5, 6.5, 7 and 6.5 respectively. All metals were poorly adsorbed at  $\text{pH} < 4$ . A previous study with Amberlite IR-120 performed by Demirbas et al. [22] concluded similar results. At low pH values,  $\text{H}^+$  ions were adsorbed on the adsorbent surface and the net positive charge was resulting in a strong attraction for negatively charged ions. On the other hand, the  $\text{OH}^-$  concentration increased on the adsorbent surface so that more free surface were obtained for the negatively charged ions resulting in the increase of removal rate [23].

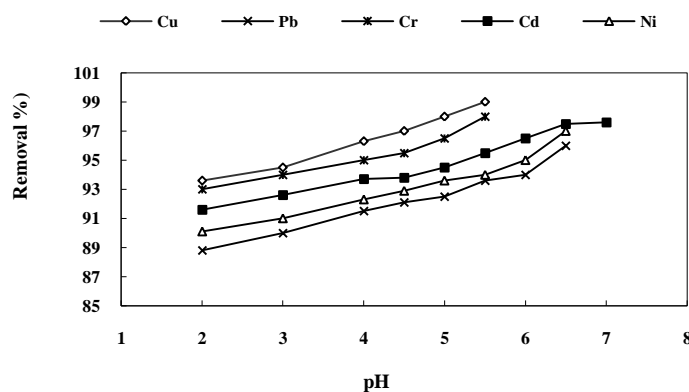


**Figure 6:** Effect of initial pH on metals removal by Mag-Dow nanocomposite

### 3.4. Effect of dose

The adsorption of metal ions increases by increasing the composite dose (Fig. 7). The adsorption of metals had the highest values using 0.5 g/L of the composite and it was taken as the optimum amount for other experiments. The increasing adsorbent dose provides more available sorption sites and high surface area. The optimum dose for Dowex resin alone is 0.8 g/L. It can be concluded that the composite gives higher metals adsorption using small amount of resin and magnetite. Increasing the adsorbent dose above 0.5 g/L have a little or no change on metals removal, as the surface area of the composite decrease as a result of the aggregation on the adsorption sites.

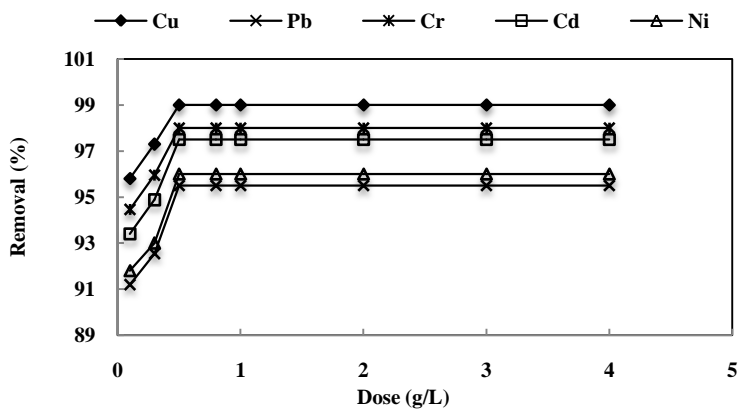


**Figure 7:** Effect of adsorbent dose on metals removal by Mag-Dow nanocomposite

### 3.5. Desorption of Metals and reusability of Mag –Dow nanocomposite

Desorption experiments were performed by mixing the metals loaded composite with a mixture of 2M NaCl and 1M NaOH for 2h. The desorption efficiency for different metals used was found to be 96 % and the regenerated

Mag-Dow nanocomposite was reused five cycles of adsorption–desorption and the results illustrate that the adsorption capacity are nearly the same as those for the fresh one.

### 3.6. Equilibrium Modeling

#### 3.6.1. Adsorption isotherms

The Freundlich adsorption isotherm [24] predicts the multilayer adsorption on heterogeneous surfaces with a non-uniform distribution of the adsorption heat over the surfaces. Eq. (2) describes Freundlich adsorption isotherm:

$$\log q_e = \log K_F + \frac{1}{n} \log C_e \quad (2)$$

$q_e$  is the adsorption capacity in equilibrium, (mg/g),  $C_e$  is the equilibrium solute phase concentration in aqueous phase in solute mass/solution volume, (mg/L).  $K_F$  is a Freundlich equation parameters and used as a relative measure for the adsorption capacity (mg/g),  $1/n$  is related to the intensity of the adsorption. Freundlich adsorption isotherm constants  $K_F$  and  $n$  were determined from the intercept and slope of a plot of  $\log q_e$  versus  $\log C_e$  (Fi. 8a). The values of Freundlich constants  $K_F$ ,  $1/n$  and the correlation coefficient of the fitting are shown in Table 2.

Isotherms with  $1/n < 1$  indicate the high affinity between both adsorbate and adsorbent and imply the presence of chemisorption reaction [25]. The values of  $1/n$  obtained in this study were observed to be less than unity and had values of 0.29, 0.4, 0.3, 0.29, 0.38 for  $Cu^{2+}$ ,  $Pb^{2+}$ ,  $Cr^{2+}$ ,  $Cd^{2+}$  and  $Ni^{2+}$  metal ions (Table 2) which indicate favorable adsorption.

The Langmuir isotherm [26] used to determine the adsorption capacity which is corresponding to monolayer adsorption on a uniform surface. The expression for the Langmuir isotherm listed in Eq.3:

$$\frac{C_e}{q_e} = \frac{1}{bq_{max}} + \frac{C_e}{q_{max}} \quad (3)$$

$q_{max}$  is maximum adsorption capacity (mg/g),  $b$  is a Langmuir constant that relates to the free energy of adsorption (L/mg). The values of  $q_{max}$  and  $b$  were determined by plotting  $C_e/q_e$  versus  $C_e$  (Fig.8b) and their values are given in Table 2. It was noted that the vales of correlation coefficient ( $R^2 \geq 0.98$ ) for Langmuir isotherm model indicated a significant correlation. It has been reported in the literature that the maximum adsorption capacity values of materials such as Fly ash [27] orange waste [28] and bone char [29] were 0.03, 48.3 and 64.1 mg/g respectively, for  $Cd^{2+}$  metal ions. Nano magnetite prepared by Sharma and Srivastava [30] had adsorption capacity value of 11.53 mg/g for  $Ni^{2+}$  metal ions. The adsorption capacity of  $Cd^{2+}$  was found to be 4.94 mg/g using hematite as stated by Singh et al. [31].

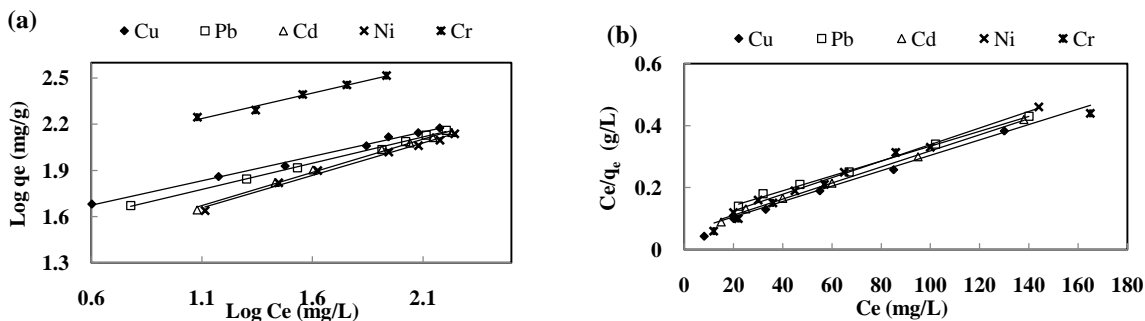


**Figure 8:** a) Freundlich b) Langmuir isotherm plots for metals adsorption by Mag-Dow nanocomposite (pH: 5.5, contact time: 30 min, shaking rate: 200 rpm, amount of adsorbent: 0.5 g/L).

Dubinin–Kaganer–Radushkevich (DKR) isotherm model is applicable for physical adsorption processes. DKR isotherm [32] can be described by Eq.4:

$$\ln q_e = \ln q_{max} - \beta \varepsilon^2 \quad (4)$$

$\beta$  is a constant which related to free energy ( $\text{mol}^2/\text{kJ}^2$ ), and  $\varepsilon$  can be calculated from equation (5):

$$\varepsilon = RT \left( 1 + \frac{1}{C_e} \right) \quad (5)$$

The mean free energy of adsorption (E) is calculated by Eq. (6):

$$E = \frac{1}{\sqrt{-2\beta}} \quad (6)$$

The DKR parameters are listed in Table 2. The magnitude of E used to characterize the adsorption by ion-exchange if its value in the range of 8–16 kJ/mol. Physical adsorption is indicated by E values < 8 kJ/mol [33]. In this study, E values obtained from Eq (6) are 11.3, 10.6, 13.7, 12.3 and 11.1 kJ/mol for Cr(VI), Ni<sup>2+</sup>, Cu<sup>2+</sup>, Cd<sup>2+</sup> and Pb<sup>2+</sup> respectively, for the adsorption on the composite. From these results the type of adsorption of the studied metal ions is defined as chemical ion exchange reactions rather than physical adsorption.

**Table 2:** Freundlich, Langmuir and DKR isothermal adsorption equation parameters for the adsorption of Cu<sup>2+</sup>, Pb<sup>2+</sup>, Cr(VI), Cd<sup>2+</sup> and Ni<sup>2+</sup> by Mag-Dow nanocomposite at room temperature ( adsorbent dose : 0.5 g/L, pH value: 5.5 , metals concentration: 100- 450 mg/L , contact time : 30 min , agitation speed: 200 rpm ).

Freundlich isotherm parameters	Cu <sup>2+</sup>	Pb <sup>2+</sup>	Cr(VI)	Cd <sup>2+</sup>	Ni <sup>2+</sup>
1/n	0.29	0.4	0.3	0.29	0.38
K <sub>F</sub> (mg/g)	91.2	44.6	81.1	79.4	50.1
R <sup>2</sup>	0.98	0.97	0.97	0.97	0.97
Langmuir isotherm parameters					
q <sub>max</sub> (mg/g)	416	380	400	398	384
b (L/mg)	0.004	0.03	0.044	0.038	0.04
R <sup>2</sup>	0.99	0.98	0.99	0.99	0.99
DKR isotherm parameters					
q <sub>max</sub> (mol /g)	0.01	6x10 <sup>-3</sup>	0.01	7.4x10 <sup>-3</sup>	0.01
E(KJ/mol)	13.7	11.1	13	12.3	10.6
R <sup>2</sup>	0.98	0.97	0.96	0.96	0.96

### 3.6.2. Adsorption kinetics

Pseudo -first-order, pseudo second-order and Elovich models were used to interpret the experimental data. The pseudo first-order equation [34] identifies the adsorption based on the sorption capacity of solids. The form of pseudo first order model is given by:

$$\log(q_e - q_t) = \log q_e - \frac{K_1 t}{2.303} \quad (7)$$

K<sub>1</sub> is the rate constant of first-order reaction model (min<sup>-1</sup>).

The calculated results of the first-order rate equation. The q<sub>e</sub> values acquired by this method which are given in Table 3, did not agree with the experimental values. So the adsorption does not follow the first-order equation model.

Second-order kinetic equation was and can be represented by the following Eq.8 [35]:

$$\frac{t}{q_t} = \frac{1}{K_2 q_e^2} + \frac{1}{q_e} t \quad (8)$$

Where k<sub>2</sub> is the second-order adsorption constant (g/mg.min). The k<sub>2</sub> and q<sub>e</sub> values were calculated from the slope and intercept of the linear plot of t/q<sub>t</sub> vs. t and are summarized in Table 3.

The correlation coefficient values of the second-order equation are high and the calculated q<sub>e</sub> values agreed well with the experimental data, which suggests that the second-order kinetics is applied and the rate limiting step in adsorption is chemisorption.

The Elovich kinetic model [36] is useful in describing adsorption on highly heterogeneous adsorbents and is expressed by equation (9):

$$q_e = \frac{1}{\beta} \ln(\alpha\beta) + \frac{1}{\beta} \ln(t) \quad (9)$$

Where α (mg/g.min) is the initial sorption rate constant and the parameter β (g/mg) is the desorption constant. The constants α and β can be obtained from the slope and intercept of the plot of q<sub>t</sub> vs ln t and are listed in Table 3. In the case of using the Elovich equation, the correlation coefficients are lower than those of the pseudo second-order equation. This situation indicates that the Elovich equation might not be sufficient to describe the mechanism which suggests that the adsorption process is very fast and probably controlled by chemical adsorption.

**Table.3.** Kinetic parameters for Cu<sup>2+</sup>,Pb<sup>2+</sup>,Cr(VI), Cd<sup>2+</sup> and Ni<sup>2+</sup> adsorption by Mag-Dow nanocomposite at room temperature (absorbent dose :0.5 g/L, pH value: 5.5 , metals concentration: 20mg/L , contact time :5-30 min , agitation speed:200 rpm ).

<b>Pseudo-first order</b>	<b>Cu<sup>2+</sup></b>	<b>Pb<sup>2+</sup></b>	<b>Cr(VI)</b>	<b>Cd<sup>2+</sup></b>	<b>Ni<sup>2+</sup></b>
<i>q<sub>e</sub></i> (mg/g)(calculated)	3.1	5.4	2.7	3.3	2.3
<i>q<sub>e</sub></i> (mg/g)(experiment)	38.7	36.5	37	37	37.5
<i>K<sub>1</sub></i> (min <sup>-1</sup> )	0.09	0.11	0.08	0.06	0.06
<i>R<sup>2</sup></i>	0.93	0.91	0.88	0.95	0.88
<b>Pseudo-second order</b>					
<i>q<sub>e</sub></i> (mg/g) (calculated)	38.9	37	37.6	37.4	38
<i>q<sub>e</sub></i> (mg/g)(experiment)	38.5	36.5	37.2	37	37
<i>K<sub>2</sub></i> (g/mgmin)	0.05	0.03	0.03	0.04	0.03
<i>R<sup>2</sup></i>	0.99	0.99	0.99	0.99	0.99
<b>Elovich kinetic model</b>					
<i>α</i> (mg/g min)	2.2x10 <sup>15</sup>	8.6x10 <sup>9</sup>	1.1x10 <sup>19</sup>	3x10 <sup>2-</sup>	3.3x10 <sup>9</sup>
<i>β</i> (g/mg)	1.01	0.7	1.2	0.9	.67
<i>R<sup>2</sup></i>	0.92	0.95	0.93	0.94	0.93

### 3.7. Treatment of wastewater

The obtained optimal parameters have been applied to wastewater from a glass factory in the industrial zone (Cairo) in order to remove the contained lead effluents. Wastewater samples were collected from the end of different plant production stages. Samples collected from one-day shift to represent the daily operations for waste. Lead concentration and pH values were measured according to APHA [19]. The steps of factory production are glazing, polishing, products sorting and final product

The sources of wastewater come from glazing and polishing steps. Table 4 shows the characteristics of waste from glazing and polishing steps. Lead concentrations were 210 mg/L from the final waste of glazing stage. In polishing stage lead concentrations decreased to 5 mg/L which is still higher than the permissible limits of the World Bank Standard for Electroplating Effluent Discharge into Surface Water (law 44 for year 2000) which allow lead concentration to be less than 1 mg/L. The prepared adsorbent Mag-Dow was used to adsorb lead at optimum conditions without pH changing in batch experiments. The removal percentage of lead using Mag-Dow was 97.5 % at the optimum conditions (dose, 0.5g/L; contact time, 30 min).

**Table 4 :** Characteristics of rinsewater obtained from glass factory

<b>Test</b>	<b>Glazing step</b>	<b>Polishing step</b>	<b>Standard law (44,year 2000)</b>
<b>pH</b>	8.5	7.9	6-9.5
<b>Turbidity (NTU)</b>	1276	52	-----
<b>Chemical Oxygen Demand COD (mg/L)</b>	1262	62	1100
<b>Total Organic Nitrogen (mg/L)</b>	9.2	4.5	100
<b>Iron (Fe) (mg/L)</b>	0.3	0.4	-----
<b>Lead (Pb) (mg/L)</b>	210	5	1

### Conclusion

Mag-Dow nanocomposite has been investigated for the removal of different metal ions from aqueous solutions. The metals adsorption was tested at different conditions such as contact time , initial pH and adsorbent dose. The adsorption was fast and attained equilibrium at 30 min using a volume of 0.5 g/L. The adsorption data followed Langmuir isotherm equation and showed absorption capacity ranging from 380 to 416 mg/g. Metal ions showed adsorption kinetics following the pseudo-second order model. the adsorbent could be easily regenerated and reused almost without loss of adsorption capacity.



## Acknowledgement

The authors gratefully acknowledge the staffs of National Research Centre (Cairo, Egypt) and heavy metals lab at Water Pollution Research Departement ,for their support .

## References

1. Ghorbel-Abid I., Galai K., Trabelsi-Ayadi M., *Desalination*. 256 (2010) 190.
2. Geise G.M., Lee H.-S., Miller D.J., Freeman B.D., McGrath J.E., Paul D.R., *J. Polym. Sci. B: Polym. Phys.* (2010) 1685–1718.
3. Madsen H.T., *Chemistry of Advanced Environmental Chemistry of Advanced Environmental Purification Processes of Water*, Elsevier, 2014, pp. 199–248.
4. Bratby J., *IWA Publishing*, London, 2006.
5. Yargeau V., in: F. Zeman (Ed.), *Metropolitan Sustainability: Understanding and Improving the Urban Environment*, Elsevier, 2012, pp. 390–405.
6. Ratnayaka D.D., Brandt M.J., Johnson K.M., in: D.D. Ratnayaka, M.J. Brandt, K.M. Johnson (Eds.), *Water Supply*, Elsevier, 2009, pp. 315–350.
7. Gupta V., Ali I., in: V. Gupta, I. Ali (Eds.), *Environmental Water: Advances in Treatment, Remediation and Recycling*, Elsevier, 2013, pp. 29–91.
8. Gupta V., Ali I., in: V. Gupta, I. Ali (Eds.), *Environmental Water: Advances in Treatment, Remediation and Recycling*, Elsevier, 2013, pp. 93–116.
9. Chen Y., Pan B., Li H., Zhang W., Lv L., Wu J., *Environ. Sci. Technol.*, 44(2010) 3508.
10. Wan L., Wang Y., Qian S., *J. Appl. Polym. Sci.* 84 (2002) 29.
11. Varma A.J., Deshpande S.V., Kennedy J.F., *Carbohydr. Polym.* 55 (2004) 77.
12. Funes A., de Vicente J., Cruz-Pizarro L., de Vicente I., *Water Res.* 53 (2014) 110–122.
13. Dias A.M.G.C., Hussain A., Marcos A.S., Roque A.C.A., *Biotechnol Adv.* 29(2011) 142.
14. Wang S., Tang J., Zhao H., Wan J., Chen K., *J. Colloid Interface Sci.* 432 (2014) 43–46.
15. Ianoş R., Păcurariu C., Mihoc G., *Ceramics International*, 40(2014) 13649–13657.
16. Atia A.A., Donia A.M., Shahin A.E., *Sep. Purif. Technol.* 46(2005) 208.
17. Ambashta R.D., Sillanpää M., *J. Hazard. Mater.* (2010) 38–49.
18. Donia A.M., Atia A.A., El-Boraey H.A., Mabrouk D., *Sep. Purif. Technol.* 49(2006) 64.
19. APHA, American Public Health Association, 2005. *Standard Methods for the Examination of Water and Wastewater*. 21<sup>st</sup> edn. Washington, DC.
20. Cattaruzza F., Fiorani D., Flamini A., Imperatori P., Scavia G., et al., *Chem Mater.* 17 (2005) 3311.
21. Pehlivan E., Altun T., *J. Hazard. Mater.* 134(2006) 149–156.
22. Demirbas A., Pehlivan E., Gode F., Altun T., Arslan G., *J. Colloid Interf. Sci.* 282(2005) 20.
23. Tewari N., Vasudevan P., Guha B.K., *Biochem. Eng. J.* 23(2005) 185.
24. Freundlich H.M.F., Over the adsorption in solution. *J. Phys. Chem.* 57(1906) 385.
25. Hameed B.H., Din A.T.M., Ahmad A.L., *J. Hazard. Mater.* 141, (2007) 819.
26. Langmuir I., *J. Am. Chem. Soc.* 38 (1916) 2221–2295.
27. Rio M., Parwate A.V., Bhole A.G., *Waste Manage.* 22(2002) 821.
28. Perez-Marin A.B., Zapata V.M., Ortuno J.F., Aguilar M., J. Saez, M. Llorens, *J. Hazard. Mater.* 139 (2007) 122.
29. Cheung C.W., Porter J.F., McKay G., *Water Res.* 35 (2001) 605.
30. Sharma Y.C., Srivastava V., *J. Chem. Eng. Data*, 55(2010) 1441.
31. Singh D.B., Rupainwar D.C., Prasad G., Jayaprakas K.C., *J. Hazard. Mater.* 60(1998) 29.
32. Hutson N.D., Yang R.T., *Adsorption*. 3(1997) 189.
33. Hao Y.-M., Chen M., Hu Z.-B., *J. Hazard. Mater.* 184(2010) 392.
34. Ho Y.S., *Scientometrics*. 59 (2004) 171.
35. Ho Y.S., *J. Hazard Mater.* 136(2006) 681.
36. Sparks D.L., 1986. In D.L. Sparks (ed) *Soil physical chemistry*, Boca Raton: CRC Press. pp 12-18.

(2017) ; <http://www.jmaterenvironsci.com>